Materials and Design 33 (2012) 563–568

Contents lists available at ScienceDirect

Materials and Design

journal homepage: www.elsevier.com/locate/matdes

Fracture toughness of a directionally solidified Al–Nb–Ni ternary eutectic

C.T. Rios [a], R.J. Contieri [b], S.A. Souza [b], A. Cremasco [b], A.O.F. Hayama [a], R. Caram [b,*]

[a] Federal University of Mato Grosso, Rondonopolis, MT 78735-910, Brazil
[b] University of Campinas, Rua Mendeleyev, 200, Campinas, SP 13083-860, Brazil

ARTICLE INFO

Article history:
Received 27 January 2011
Accepted 30 April 2011
Available online 9 May 2011

Keywords:
A. Metal matrix composites
E. Fracture
F. Microstructure

ABSTRACT

Fracture toughness (K_{IC}), an important property of brittle materials, can be determined by indentation cracking tests. This paper reports on an investigation of the fracture toughness of a directionally solidified Al_3Nb–Nb_2Al–AlNbNi ternary eutectic, based on the Vickers indentation test applied to longitudinal and transverse sections of its microstructure. The measurements were taken using indentation loads varying from 2.45 to 24.5 N. Correlations between the resulting crack parameters and indentation load were evaluated using Palmqvist and half-penny cracks models. In the range of indentation loads studied, the results suggested that the Palmqvist model provided a better fit to the experimental data. Fracture toughness was calculated using equations developed for Palmqvist crack mode. The indentation fracture toughness values for longitudinal and transverse sections are in the range of 2.82–3.05 MPa $m^{1/2}$ and 2.98–3.59 MPa $m^{1/2}$, respectively. It was found that the addition of Ni and incorporation of a third phase to the Al_3Nb–Nb_2Al eutectic improved fracture toughness of this *in situ* composite material.

1. Introduction

In situ composite materials produced by directional solidification of high temperature eutectic alloys have been the subject of a number of investigations, usually aiming to replace Ni-based alloys in high temperatures applications [1]. This type of composite is composed of two or more phases, usually intermetallic phases, with the reinforcing phases produced during the manufacturing process [2]. Research has recently focused on the Al_3Nb–Nb_2Al eutectic alloy for the manufacture of eutectic-based structural composites. This eutectic material shows high strength at elevated temperatures, but poor fracture toughness at low temperatures [3,4]. Fracture toughness or the critical stress intensity factor, K_{IC}, is essential for predicting the mechanical behavior of brittle materials such as intermetallic compounds [5].

An interesting way to determine K_{IC} is by the Vickers hardness indentation technique [6–8]. This method was first examined as a tool to describe fracture toughness in the 1950s [7]. The application of certain indentation loads will nucleate cracks in brittle materials, which may be correlated to fracture toughness. In such cases, two types of indentation cracks occur, depending on their geometrical features: Palmqvist cracks and radial-median cracks [9,10].

Palmqvist cracks consist of four half-penny-shaped cracks that initiate only at the corners of the indentation, their extensions are restricted to small distances beneath the surface and they show a propensity to be just as deep as the indentation. On the other hand, radial-median cracks, also called half-penny cracks, consist of two fully developed semi-elliptical cracks that commence at the corners of the indentation [11–13]. They develop under and around the indentation, penetrating far below the surface and forming cracks normal to the indentation plane. Details of both these crack modes, including their dimensions, are illustrated in Fig. 1 [6–10].

It is well known that the phase arrangement in a eutectic microstructure controls its mechanical behavior. An earlier study found that adding Ni to the binary Al_3Nb–Nb_2Al eutectic led to a ternary eutectic transformation ($L \leftrightarrows Al_3Nb + Nb_2Al + AlNbNi$) at Al–40.4Nb–2.42Ni (at.%) [14] and application of directional solidification to this ternary eutectic resulted in a very regular microstructure composed of fiber-like phases [15]. It is possible that the incorporation of a third phase to the Al_3Nb–Nb_2Al eutectic may positively alter fracture toughness of this *in situ* composite material.

To address questions pertaining to the effect of an additional phase on mechanical behavior of the Al_3Nb–Nb_2Al eutectic, this paper presents the results of the Vickers indentation of directionally solidified $Al_3Nb + Nb_2Al + AlNbNi$ ternary eutectic and discusses correlations between the microstructure and fracture toughness.

2. Experimental procedure

The ternary eutectic alloy in the Al–Nb–Ni system was prepared with appropriate amounts of pure elements melted in an arc furnace equipped with a vacuum system combined with injection of

* Corresponding author. Tel./fax: +55 19 35213314.
E-mail address: rcaram@fem.unicamp.br (R. Caram).

0261-3069/$ - see front matter © 2011 Elsevier Ltd. All rights reserved.
doi:10.1016/j.matdes.2011.04.064

high purity argon. Ternary eutectic samples were solidified directionally using the Bridgman technique under an argon atmosphere. The 30-mm-long, 6.0-mm-diameter ingots were placed in high purity Al_2O_3 crucibles and solidified by slowly moving the crucible from the upper hot region to the lower cold region, at a thermal gradient ranging from 80 to 100 °C/cm, with a growth rate of 1.0 cm/h.

Normal metallographic preparation procedures were utilized to investigate the microstructure. Chemical etching consisted of 10 vol.% HF, 30 vol.% HNO_3 and 60 vol.% lactic acid. The material was microanalyzed by optical microscopy (OM) (Olympus – BX60M) and scanning electron microscopy (SEM) (Jeol JXA 840A). Indentation tests were carried out on longitudinal and transverse sections of a directionally solidified sample, using a W-Testor hardness indenter under 2.45 N (250 gf), 4.9 N (500 gf), 7.35 N (750 gf), 9.8 N (1000 gf), 14.7 N (1500 gf) and 24.5 (2500 gf) applied for 15 s. A sequence of eight measurements was taken of each load.

Elastic behavior of directionally solidified ternary eutectic was evaluated by using pulse-echo ultrasonic echography technique. The diagram in Fig. 2 shows the experimental apparatus used for measuring the elastic constants. Piezoelectric transducers (5 MHz) in contact with the specimen were used to determine longitudinal V_L and transversal V_T velocities of sound waves in the material. The density (ρ) of the samples was determined by the Archimedes method. These velocities, density and geometrical features of the samples were used to determine Young's modulus (E), shear modulus (G) and Poisson's ratio (υ). They were determined according to the following equations [16,17]:

$$E = \frac{\rho V_T^2\left(3V_L^2 - 4V_T^2\right)}{V_L^2 - V_T^2} \quad (1)$$

$$G = \rho V_T^2 \quad (2)$$

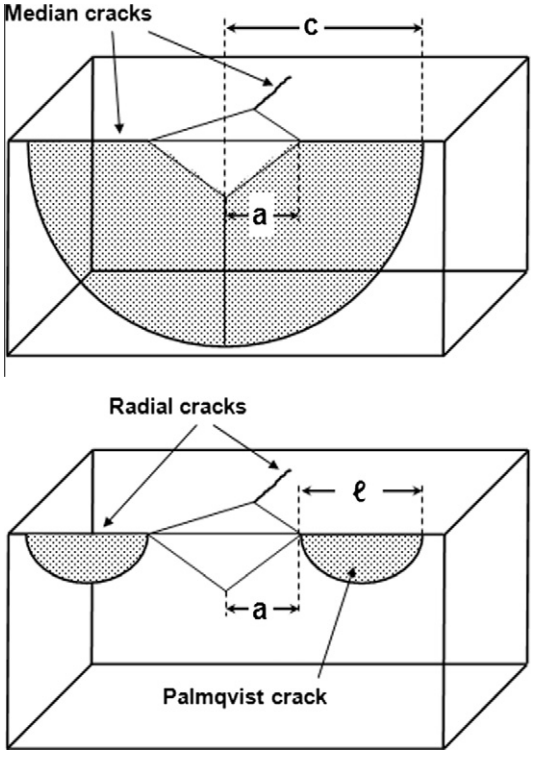

Fig. 1. Top and transverse views of the Palmqvist and Radial-median crack modes induced by Vickers indentation.

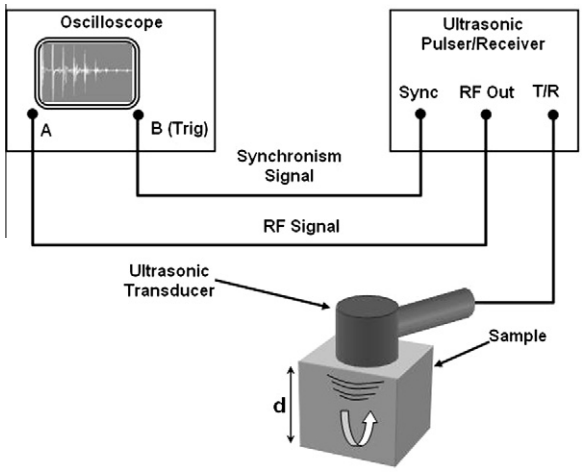

Fig. 2. Diagram of the experimental apparatus for measuring elastic constants.

$$\upsilon = \frac{E}{2G} - 1 \quad (3)$$

Crack mode evaluation and a 3D reconstruction of the eutectic microstructure were carried out by obtaining metallographic images at several planes in the 3D domain. This procedure is the so-called serial sectioning technique and involves removing a certain amount of materials by polishing samples containing Vickers hardness indentations, followed by recording of the metallographic plane. Repeating this procedure a number of times generates a significant amount of 3D information of the eutectic microstructure. The Vickers indentations were also utilized to align images of each plane with the images of the preceding metallographic plane. In this study, a sectioning depth of 4.0 μm was chosen [18].

3. Results and discussion

Fig. 3a depicts a three-dimensional reconstruction of the phase arrangements of the Al_3Nb–Nb_2Al–AlNbNi ternary eutectic obtained by directional solidification using the serial sectioning technique. The reconstructed microstructure suggests that the phases are continuous in the growth direction and present some sinuosity. It is a complex task to make a complete identification of the constituent phases of the Al_3Nb–Nb_2Al–AlNbNi ternary eutectic microstructure under an optical microscope, since optical microscopy does not suffice to identify the AlNbNi phase [14]. On the other hand, the use of SEM (backscattered electron images)

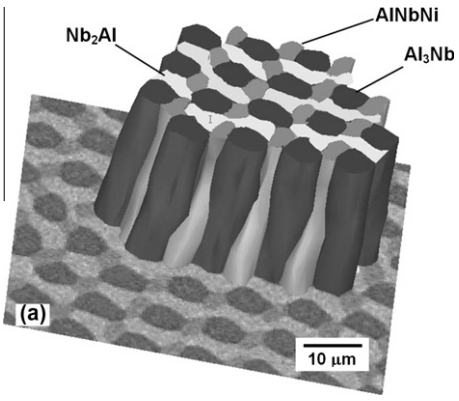

Fig. 3a. Three-dimensional reconstruction of the Al_3Nb–Nb_2Al–AlNbNi ternary eutectic structure.

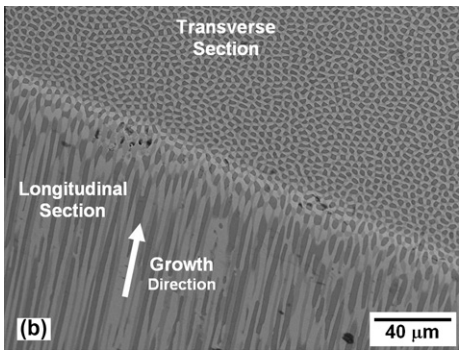

Fig. 3b. SEM image, backscattered electron, showing longitudinal and transverse sections of a directionally solidified Al_3Nb–Nb_2Al–AlNbNi ternary eutectic sample.

revealed the third phase, as indicated in Fig. 3b, which shows longitudinal and transverse microstructures of a directionally solidified Al_3Nb–Nb_2Al–AlNbNi ternary eutectic sample.

The micrographs in Fig. 4 show indentation on the directionally solidified Al–Nb–Ni ternary eutectic alloy produced by a 9.8 N load. The ultrasonic velocity measurements indicated that Poisson's ratio, v, of the ternary eutectic is 0.269 and Young's modulus is 251 GPa. Additionally, the density was measured and the value found was 5.38 g/cm^3.

As mentioned before, Vickers indentation produces cracks that are classified into two types, i.e., Palmqvist and half-penny crack systems. A rough guide to identify the crack system resulting from Vickers indentation is by evaluating the ratios of c/a or ℓ/a ($\ell/a = c/a - 1$). According to Fig. 1, a is the indentation half-diagonal length, c is surface radial crack length and ℓ is the crack length at the indentation corners [5–11]. According to Niihara et al. [9], the crack system changes from Palmqvist system to half-penny system as the indentation load increases. If the relation between the crack length and the half diagonal length, c/a, is >2.5, the crack system is classified as half-penny cracks [10]. However, if ratio $c/a < 2.5$, the crack system is of Palmqvist type [16].

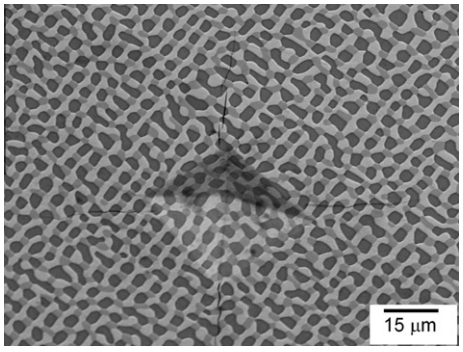

Fig. 4. Micrograph with Vickers indentation on a directionally solidified Al–Nb–Ni ternary eutectic (SEM backscattered electrons images).

Table 1 presents the average values of indentation parameters a, c and ℓ as a function of indentation load. These values, which were identified on the longitudinal and transverse sections of a directionally solidified Al–Nb–Ni ternary eutectic, suggest that Palmqvist crack is the predominant crack mode in all the case studied.

An additional approach to differentiate between the two types is by analyzing the relationship between indentation parameter and indentation load [19]. In case of Palmqvist crack system, the relationship between indentation load, P, and the crack length is given by the crack resistance [20,21]. The crack resistance, W, is defined by the relationship between indentation load, P, and the sum of the crack lengths, ℓ [19]:

$$W = \frac{P}{4\bar{\ell}} \tag{4}$$

where $\bar{\ell}$ is the average crack length. In order to account for the surface finish, a modification of Eq. (4) is given by [19,22,23]:

$$W = \frac{P - P_0}{4\bar{\ell}} \tag{5}$$

where P_0 is the threshold load to initiate cracking [5].

Fig. 5, which depicts the evolution of crack length versus indentation load, indicates that both longitudinal and transverse section samples follow a linear relationship between P and $\bar{\ell}$, given by Eq. (5). W_L (longitudinal section) was found to be near 0.118 MN m^{-1}, while W_T (transverse section) was close to 0.165 MN m^{-1}. The value of P_0 is found to be −0.047 N and −0.549 N for longitudinal and transverse sections, respectively.

According to Fig. 1, $c = \ell + a$ and considering that H is the indentation pressure, which is given by $P/2a^2$, c can be written as [19]:

$$c = \bar{\ell} + a = \frac{P - P_0}{4W} + \left(\frac{P}{2H}\right)^{1/2} \tag{6}$$

Fig. 6 presents a comparison between experimental data and predictions of Eq. (6) for crack dimension versus indentation load. Following a similar procedure reported by Shetty et al. [19], the first term of Eq. (6) was obtained from the best-fit equations for Palmqvist crack dimension versus indentation load and the second term was found by obtaining the best fit equations for the indentation half-diagonal length versus indentation load, which is seen in Fig. 7.

In case of half-penny cracks, the relationship between indentation load and crack length can be given by the model proposed by Lawn and Fuller [24]:

$$c = kP^{2/3} \tag{7}$$

where k is a constant that depends on hardness, elastic modulus, indenter geometry and fracture toughness [19]. Fig. 8 shows the evolution of crack length given by Eq. (7) as a function of indentation load. By observing Figs. 6 and 8, one may conclude that the

Table 1
Indentation parameters as a function of indentation load on longitudinal and transverse sections of a directionally solidified Al–Nb–Ni ternary eutectic.

Load N (gf)	Longitudinal section				Transverse section			
	$d = 2a$ (μm)	ℓ (μm)	c (μm)	c/a	$d = 2a$ (μm)	ℓ (μm)	c (μm)	c/a
2.45 (250)	23.5 ± 0.4	5.2 ± 0.5	17.0 ± 0.6	1.4 ± 0.0	23.0 ± 0.4	4.8 ± 0.8	16.4 ± 0.9	1.4 ± 0.1
4.90 (500)	32.9 ± 0.6	11.3 ± 1.8	27.8 ± 5	1.7 ± 0.1	327 ± 0.5	8.2 ± 0.8	24.6 ± 0.8	1.5 ± 0.1
7.35 (750)	40.8 ± 0.4	16.7 ± 1.9	37.1 ± 2.0	1.8 ± 0.1	–	–	–	
9.8 (1000)	47.4 ± 0.4	20.3 ± 2.1	44.0 ± 2.3	1.9 ± 0.1	47.0 ± 0.3	16.6 ± 2.8	40.1 ± 2.8	1.7 ± 0.1
14.7 (1500)	58.6 ± 0.4	29.8 ± 2.5	59.1 ± 2.5	2.0 ± 0.1	58.1 ± 0.3	20.8 ± 0.9	49.9 ± 0.9	1.7 ± 0.0
24.5 (2500)	75.7 ± 0.3	52.3 ± 2.7	90.2 ± 2.7	2.4 ± 0.1	75.5 ± 0.3	41.1 ± 1.9	78.9 ± 1.9	2.0 ± 0.1

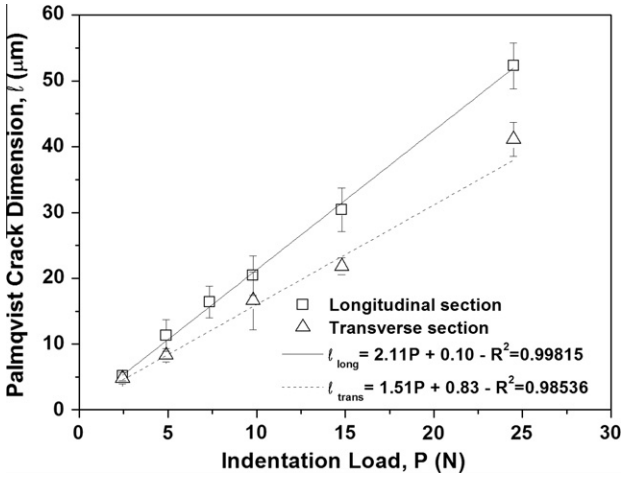

Fig. 5. Evolution of Palmqvist crack length as a function of indentation load on longitudinal and transverse sections of a directionally solidified Al–Nb–Ni ternary eutectic.

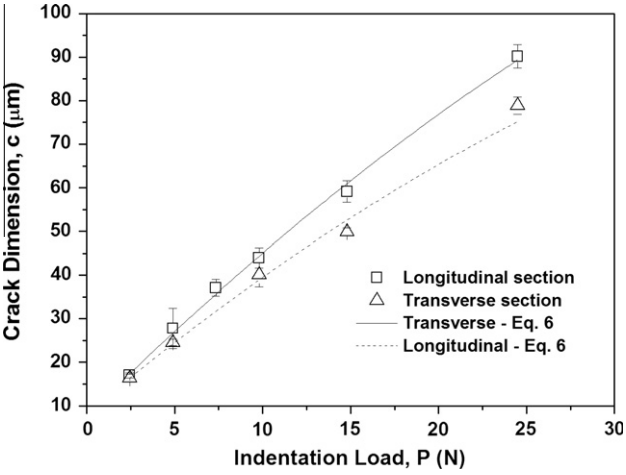

Fig. 6. Comparison between experimental data and predictions of Eq. (6) for crack dimension versus indentation load for longitudinal and transverse sections of the directionally solidified ternary eutectic.

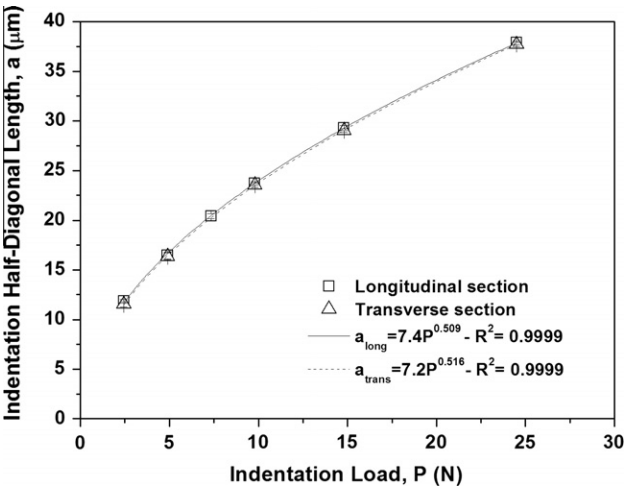

Fig. 7. Indentation half-diagonal length versus indentation load for longitudinal and transverse sections of the directionally solidified ternary eutectic.

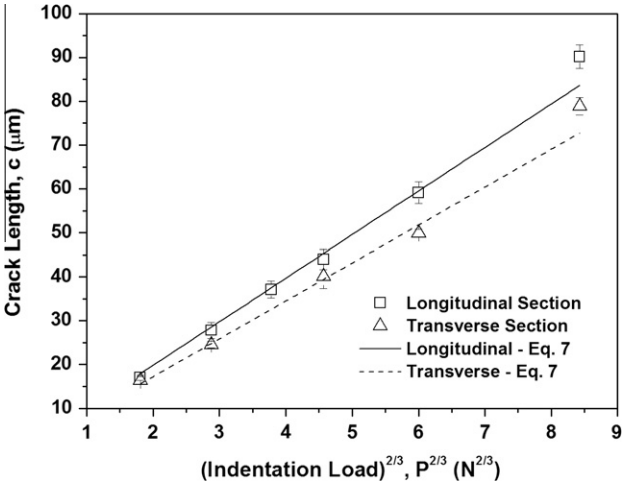

Fig. 8. Evolution of crack length as a function of (indentation load)$^{2/3}$ on longitudinal and transverse sections of a directionally solidified Al–Nb–Ni ternary eutectic.

experimental data indicate that the Palmqvist model shows a reasonable linear correlation between indentation parameters and indentation load. The use of the half-penny model suggested that the same experimental data does not follow a linear dependence on $P^{2/3}$.

To determine the crack mode of the directionally solidified ternary eutectic, serial sectioning of the indentation region was also applied. Fig. 9 presents metallographic images (SEM) at several planes of a 9.8 N Vickers indentation. The images were obtained by removing some amount of material by polishing the sample. Fig. 9a shows the original Vickers indentations containing radial cracks. As the sample is polished and the material is removed, the crack undergoes a size decrease, making it farther from the original indentation. Analysis of Fig. 9b allows one to verify that the crack does not extend under the indentation and hence, it is not of the radial-median type. As the polishing continues and the indentation almost disappeared, as seen in Fig. 9c, the crack size is reduced to a very small fraction of its initial size. Certainly, additional polishing will eliminate this crack completely. Again, these findings led to the inference that the crack system of this ternary eutectic is of the Palmqvist type. In a recent study, the fracture toughness of an $Al_3Nb + Nb_2Al + AlNbNi$ ternary eutectic in the as-cast condition was evaluated by Vickers indentation [25]. Correlations between the resulting crack parameters and indentation load suggested that the radial-median model resulted in a better fit to the experimental data. As the indentation load was increased, it appears that a transition from the Palmqvist to the radial-median system occurred.

Two basic approaches are frequently used to relate Vickers indentation parameters and fracture toughness of Palmqvist crack systems [8,26–28], i.e., equations of Niihara et al. [9] and Shetty et al. [19]. The equation proposed by Niihara et al. [9] is given by:

$$K_{IC} = 0.0089\left(\frac{E}{H_V}\right)^{2/5}\frac{P}{(a\ell^{1/2})} \tag{8}$$

Based on a previous study also conducted by Niihara [10], Shetty et al. [19] suggested that Vickers indentation parameters and fracture toughness is written as:

$$K_{IC} = \frac{1}{3(1-\upsilon^2)(2^{1/2}\pi^{5/2}\tan\varphi)^{1/3}}\left(H_V\frac{P}{4\ell}\right)^{1/2} \tag{9}$$

where the angle of the opposite faces of Vickers pyramid, 2φ, is equal to 136°. Considering that the ternary eutectic has $\upsilon = 0.269$, Eq. (9) can also be written as:

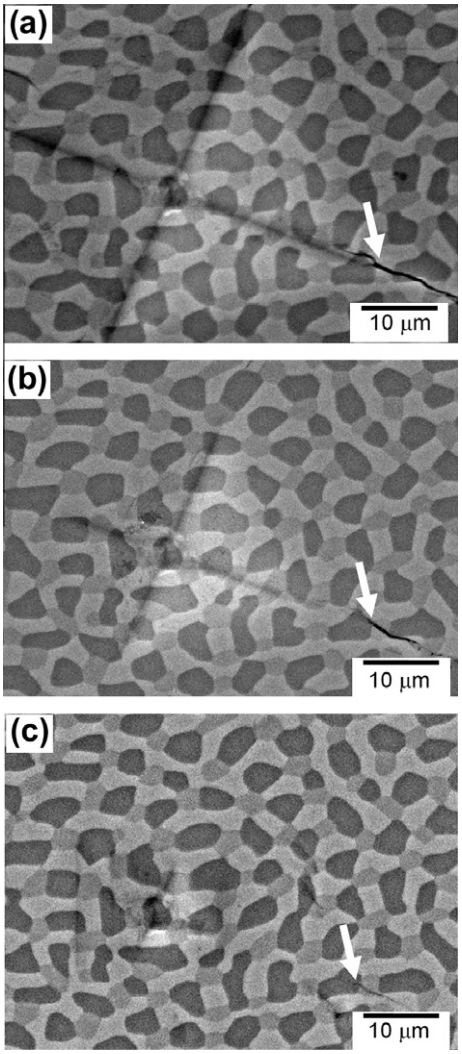

Fig. 9. Micrographs of Vickers indentations using a load of 9.8 N: (a) original Vickers indentation, (b) as the sample is polished and the material is removed, the crack undergoes a size decrease, making it farther from the original indentation and (c) as the polishing continues and the indentation almost disappeared.

$$K_{IC} = 0.0095\left(H_V \frac{P}{4\ell}\right)^{1/2} \quad (10)$$

Table 2 presents fracture toughness values calculated by applying Eqs. (8) and (10). An evaluation of these data shows that the Vickers test on longitudinal and transverse sections of a directionally solidified Al–Nb–Ni ternary eutectic resulted in values of fracture toughness for transverse and longitudinal sections, respectively, in the range of 2.82–3.05 MPa $m^{1/2}$ and 2.98–3.59 MPa $m^{1/2}$. These values are in reasonable agreement with the ones found in the literature. According to Ebrahimi et al. [29], K_{IC} for Nb_2Al is 1.9 MPa $m^{1/2}$, while Schneibel et al. [30] reported a value of 2.5 MPa $m^{1/2}$ for Al_3Nb intermetallic compound. A comparison between the fracture toughness values of the directionally solidified Al–Nb–Ni ternary eutectic and the values of the Al_3Nb–Nb_2Al eutectic [3] shows that the incorporation of the AlNbNi phase to this eutectic microstructure increased the fracture toughness.

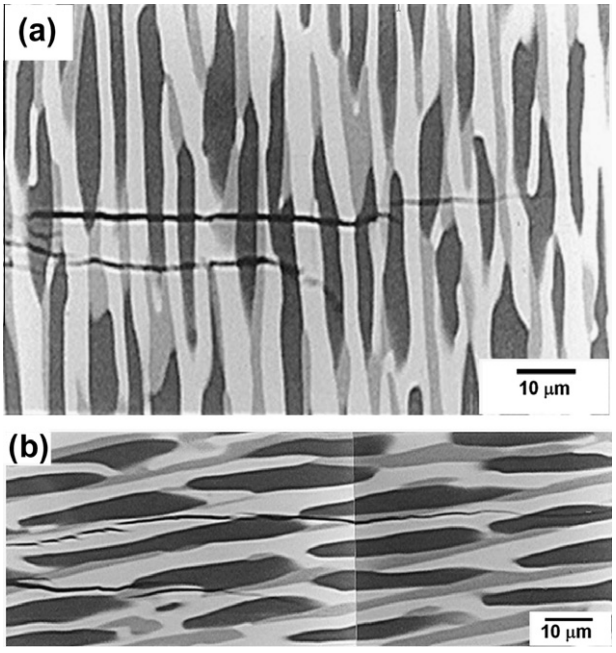

Fig. 10. Crack development in a directionally solidified Al–Nb–Ni ternary eutectic: (a) in a longitudinal section, and (b) in a transverse section.

This finding was also supported by fracture analysis of the ternary eutectic. Fig. 10 shows the morphologies of cracks resulting from the Vickers indentation as a consequence of internal stress in the bulk material. The material showed no sign of ductility or dimple formation and the cracks clearly followed a straight path, as shown in Fig. 10a. These findings suggest that the cracks do not follow grain boundaries and that the fracture is of the transgranular type. In addition, Fig. 10b leads one to conclude that the cracks move almost towards the three phases, regardless of the type of phase. This detail reveals that there is no significant difference in the fracture toughness of Nb_2Al, Al_3Nb and AlNbNi compounds. However, based on an analysis of the same microstructure, it seems that AlNbNi phase (gray phase) causes the crack to deviate slightly from its original path and hence, it acts apparently as a reinforcement of this *in situ* composite.

Fig. 11 shows the fracture surface (transverse section) of the directionally solidified Al–Nb–Ni ternary eutectic. As can be seen, this surface seems to be flat, with no sign of deformation, which suggests the occurrence of cleavage.

Table 2
Fracture toughness obtained from Eqs. (8) and (10).

Load, N (gf)	$K_{IC} = 0.0089\left(\frac{E}{H_v}\right)^{2/5}\frac{P}{a^{\ell 1/2}}$ (MPa $m^{1/2}$)		$K_{IC} = 0.0095\left(H_v \frac{P}{4\ell}\right)^{1/2}$ (MPa $m^{1/2}$)	
	Longitudinal section	Transverse section	Longitudinal section	Transverse section
2.45 (250)	2.97 ± 0.21	3.05 ± 0.31	2.97 ± 0.23	3.17 ± 0.35
4.90 (500)	2.82 ± 0.32	3.2 ± 0.21	2.91 ± 0.34	3.39 ± 0.23
7.35 (750)	2.83 ± 0.21	–	2.89 ± 0.23	–
9.8 (1000)	2.92 ± 0.20	3.27 ± 0.41	2.98 ± 0.22	3.38 ± 0.42
14.7 (1500)	2.91 ± 0.17	3.50 ± 0.11	2.96 ± 0.19	3.59 ± 0.11
24.5 (2500)	2.85 ± 0.09	3.21 ± 0.10	2.89 ± 0.09	3.28 ± 0.10

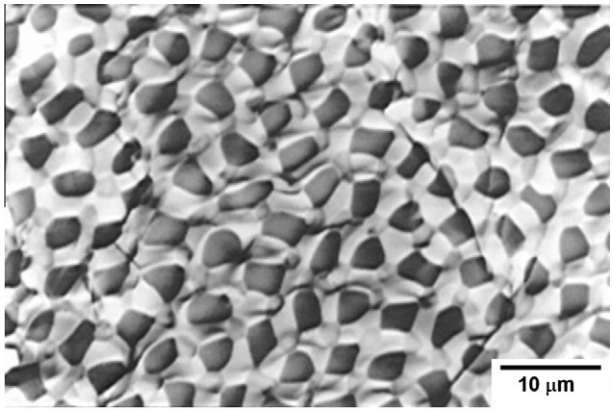

Fig. 11. Fracture surface in a directionally solidified Al–Nb–Ni ternary eutectic (transverse section).

4. Conclusions

The fracture toughness of a directionally solidified ternary eutectic in the Al-Nb-Ni system consisting of Al_3Nb, Nb_2Al and AlNb-Ni intermetallic phases was investigated using Vickers indentations on longitudinal and transverse sections. The measurements were taken with indentation loads varying from 2.45 to 24.5 N. In the range of indentation loads studied, correlations between the resulting crack parameters and indentation load suggested that the Palmqvist model provided a better fit to the experimental data. K_{IC} was calculated using Niihara et al. [9] and Shetty et al.'s [19] models. The fracture toughness values for longitudinal and transverse sections are in the range of 2.82–3.05 MPa $m^{1/2}$ and 2.98–3.59 MPa $m^{1/2}$, respectively. The elastic constants of this ternary eutectic were measured to determine the K_{IC} values. The results of these measurements indicated a Poisson's ratio, υ, of 0.269 and Young's modulus of 251 GPa. A comparison between the fracture toughness values of the directionally solidified Al–Nb–Ni ternary eutectic and the values of the Al_3Nb–Nb_2Al eutectic [3] shows that the incorporation of the AlNbNi phase to this eutectic microstructure increased the fracture toughness of the resulting structure. Finally, the fracture surface analysis led to the conclusion that transgranular fracturing occurred as a result of Vickers indentation.

Acknowledgments

The authors gratefully acknowledge the Brazilian research funding agencies FAPESP (State of São Paulo Research Foundation) and CNPq (National Council for Scientific and Technological Development) for their financial support of this work.

References

[1] Bei H, Pharr GM, George EP. A review of directionally solidified intermetallic composites for high-temperature structural applications. J Mater Sci 2004;39:3975–84.
[2] Aikin Jr RM. The mechanical properties of *in situ* composites. J Metals 1997;49:35–9.
[3] Rios CT, Ferrandini P, Caram R. Fracture toughness of the eutectic alloy Al_3Nb–Nb_2Al. Mater Lett 2003;57:3949–53.
[4] Rios CT, Milenkovic S, Caram R. Directional growth of Al–Nb–X eutectic alloys. J Cryst Growth 2000;211:466–70.
[5] Liang KM, Orange G, Fantozzi G. Evaluation by indentation of fracture toughness of ceramic materials. J Mater Sci 1990;25:207–14.
[6] Song YK, Varin RA. Indentation microcracking and toughness of newly discovered ternary intermetallic phases in the Ni–Si–Mg system. Intermetallics 1998;6:379–93.
[7] Ponton CB, Rawlings RD. Vickers indentation fracture toughness test. Part 1: Review of the literature and formulation of standardized indentation toughness equations. Mater Sci Technol 1989;5:865–72.
[8] Ponton CB, Rawlings RD. Vickers indentation fracture toughness test. Part 2: Application and critical evaluation of standardized indentation toughness equations. Mater Sci Technol 1989;5:961–75.
[9] Niihara K, Morena R, Hasselman DPH. Evaluation of K_{IC} of brittle solids by the indentation method with low crack-to-indent ratios. J Mater Sci 1982;1:13–6.
[10] Niihara K. A fracture mechanics analysis of indentation-induced Palmqvist crack in ceramics. J Mater Sci Lett 1983;2:221–3.
[11] Chicot D, Duarte G, Tricoteaux A, Jorgowski B, Leriche A, Lesage J. Vickers indentation fracture (VIF) modeling to analyze multi-cracking toughness of titania, alumina and zirconia plasma sprayed coatings. Mater Sci Eng A 2009;527:65–76.
[12] Li Z, Ghosh A, Kobayashi AS, Bradt RC. Indentation fracture toughness of sintered silicon carbide in the Palmqvist crack regime. J Am Ceram Soc 1989;72:904–11.
[13] Tsai K-M, Hsieh C-Y, Lu H-H. Sintering of binderless tungsten carbide. Ceram Int 2010;36:689–92.
[14] Rios CT, Milenkovic S, Caram R. A novel ternary eutectic in the Nb–Al–Ni system. Scripta Mater 2003;48:1495–500.
[15] Rios CT, Milenkovic S, Gama S, Caram R. Influence of the growth rate on the microstructure of a Nb–Al–Ni ternary eutectic. J Cryst Growth 2002;237–239:90–4.
[16] Keryvin V, Hoang VH, Shen J. Hardness, toughness, brittleness and cracking systems in an iron-based bulk metallic glass by indentation. Intermetallics 2009;17:211–7.
[17] Li P, Hao J, Zhao J, Duan H. The influence of ageing treatment on the microstructure and the elastic modulus of Ti27Nb8Zr alloy. Mater Sci Eng A 2010;527:7469–74.
[18] Contieri RJ, Rios CT, Zanotello M, Caram R. Growth and three-dimensional analysis of the Nb–Al–Ni ternary eutectic. Mater Charact 2008;59:693–9.
[19] Shetty DK, Wright IG, Mincer PN, Clauer H. Indentation fracture of WC–Co cermets. J Mater Sci 1985;20:1873–82.
[20] Exner HE. The influence of sample preparation on Palmqvist method for toughness testing of cemented carbides. Trans TMS AIME 1969;245:677–83.
[21] Exner EL, Pickens JR, Gurland J. A comparison of indentation crack resistance and fracture toughness of five WC–Co alloys. Metall Trans A 1978;9:736–8.
[22] Ogilvy IM, Perrott CM, Suiter JW. On the indentation fracture of cemented carbide part 1 – survey of operative fracture modes. Wear 1977;43:239–52.
[23] Perrott CM. On the indentation fracture of cemented carbide II – the nature of surface fracture toughness. Wear 1978;47:81–91.
[24] Lawn BR, Fuller R. Equilibrium penny-like cracks in indentation fracture. J Mater Sci 1975;10:2016–24.
[25] Rios CT, Coelho AA, Batista WW, Gonçalves MC, Caram R. ISE and fracture toughness evaluation by Vickers hardness testing of an Al_3Nb–Nb_2Al–AlNbNi *in situ* composite. J Alloys Compd 2009;472:65–70.
[26] Campos I, Rosas R, Figueroa U, VillaVelázquez C, Menezes A, Guevara A. Fracture toughness evaluation using Palmqvist crack models on AISI 1045 borided steels. Mater Sci Eng A 2008;488:562–8.
[27] Lin C-M, Chang C-M, Chen J-H, Wu W. Hardness, toughness and cracking systems of primary $(Cr,Fe)_{23}$ C_6 and $(Cr,Fe)_7$ C_3 carbides in high-carbon Cr-based alloys by indentation. Mater Sci Eng A 2010;527:5038–43.
[28] Wu P, Zheng Y, Zhao Y, Yu H. Effect of SiC whisker addition on the microstructures and mechanical properties of Ti(C,N)-based cermets. Mater Des 2011;32:951–6.
[29] Ebrahimi F, Hoelzer TD. Fracture toughness of $\sigma + x$ microstructures in the Nb–Ti–Al system. Mater Sci Eng A 1993;171:35–45.
[30] Schneibel HJ, Becher FP, Horton AJ. Microstructure and fracture toughness of powder processed Al_3Nb. J Mater Res 1988;3:1272–5.